Journal of Magnetic Resonance 199 (2009) 104–110

Contents lists available at ScienceDirect

Journal of Magnetic Resonance

journal homepage: www.elsevier.com/locate/jmr

Communication

Impedance matching with an adjustable segmented transmission line

Chunqi Qian *, William W. Brey

Center for Interdisciplinary Magnetic Resonance, National High Magnetic Field Laboratory, 1800 E. Paul Dirac Dr, Tallahassee, FL 32310, USA

ARTICLE INFO

Article history:
Received 26 November 2008
Revised 23 March 2009
Available online 11 April 2009

Keywords:
Impedance matching
Reflection coefficient
Transmission line segment
Resonator
Dielectric slug

ABSTRACT

A capability for impedance matching between the RF probe and the spectrometer is a standard requirement for NMR. Both lumped element and branched transmission line methods are widely used for this purpose. Here, we propose to use the segmented transmission line structure which is well known in wireless communications. It relies upon reflections between transmission lines of different characteristic impedances that are serially connected to match the impedance of a coil or resonator to the characteristic impedance of the NMR spectrometer. In our implementation, two quarter wave length dielectric slugs are placed within a coaxial transmission line. Adjustment of the positions of the slugs allows the variable tuning and matching needed for NMR probes, eliminating the need for variable capacitors and inductors. As a demonstration of the usefulness of this approach, we have incorporated a variable segmented transmission line into a home-built Variable Angle Spinning probe. Finally, we discuss the range of possible application for segmented transmission line networks in NMR probe design.

1. Introduction

Impedance matching [1] is one of the most important concepts in magnetic resonance engineering. It ensures that power extracted from the precessing magnetization of the sample is efficiently transferred from the probe to the spectrometer to optimize the detection sensitivity. Impedance matching is also needed to convert the transmit power produced by the RF amplifier into a strong rotating magnetic field B_1 within the sample coil. Many different circuits have been proposed for impedance matching to an RF sample coil in an NMR probe. The most widely known may be the L-network of two adjustable capacitors [2–5]. A "tuning" capacitor in parallel with the coil cancels the inductive reactance of the coil, and a series "matching" capacitor steps down the impedance to match the characteristic impedance of the spectrometer, which is normally 50 Ω. The presence of two independent adjustments, which is a common element in matching networks, reflects the need to control both the real and imaginary parts of the impedance presented to the spectrometer. The widespread availability of good nonmagnetic variable capacitors is an important reason for their popularity, but there is a tradeoff between capacitor size and breakdown voltage that works against their use at near microwave frequencies. Adjustable capacitors are often buffered by fixed capacitors or otherwise protected from the highest voltages in the probe circuit, but generally at a significant cost to reduced tuning or matching range.

Transmission lines have often been employed in NMR probes as impedance transformers to allow single coils to be used for multiple nuclei at multiple frequencies [6–8]. The transmission line elements are used to provide impedance matching and to improve isolation between the various channels in the probe. Here, the length of the transmission lines can be used to allow the adjustable capacitors to be located remotely from the sample coil, which is often advantageous [9,10]. While adjustable transmission lines have been used in some cases [11], most often commercial capacitors are the adjustable elements. The "Apex" (A. Palmer) and related commercial designs (Varian Inc.) are based on concentric coaxial capacitors that exhibit some transmission line behavior [12]. Tuning and matching adjustments are carried out by inserting or withdrawing sleeves of dielectric material between the shield and inner conductor. These coaxial capacitors withstand high voltages and have been shown to have low loss [12]. The mechanical implementation requires close tolerances and the electrical design requires computer simulation of the network because of transmission line effects and inductance in the adjustable capacitors. Also, segmented transmission lines employing a single dielectric slug have been incorporated into solid state NMR probes developed at Bruker Biospin, Inc.

Here, we propose a method of adjustable impedance matching based on a coaxial transmission line within which two quarter wave dielectric slugs can be independently positioned. The line can be thought of as a series of four connected transmission lines, two of which have a lower characteristic impedance due to the presence of the dielectric slugs. By changing the positions of dielectric slugs, the lengths of two of the transmission line segments can be changed and the voltage reflection at the input point can be

* Corresponding author. Fax: +1 850 644 1366.
E-mail address: qian@magnet.fsu.edu (C. Qian).

1090-7807/$ - see front matter © 2009 Elsevier Inc. All rights reserved.
doi:10.1016/j.jmr.2009.04.005

minimized by the proper cancellation of internal reflections. Tuners based on this principle are used commercially for automatic testing of power amplifiers, where they are known as "double slug" or "interferometric" load-pull tuners, and the slugs are typically driven by computer-controlled motors [13]. The basic structure is derived from the stepped transformer [14] which has long been used in wireless communication. There are obvious attractive features of the adjustable segmented line—it requires no adjustable capacitors, and it has no sliding contacts that might wear. Its long cylindrical shape fits nicely into the bore of an NMR magnet. But as we will show, this tuner has advantageous electrical properties as well. It is capable of matching a very wide range of loads, both inductive and capacitive, unlike the L-networks used in both lumped element and fixed-length transmission line probes. This interesting feature has allowed us to interchange the sample detector easily without modifications to the tuning circuit, so that the same probe body can be used with different sample coils.

In this communication, we will first go through the principles of segmented transmission lines, deriving formulas to predict the required position of the tuning slugs and the power efficiency for a given load. We will then describe how this design has been incorporated into our variable angle spinning (VAS) probe [15] and compare the performance with conventional matching networks. Finally, we will explore the potential applications of the segmented transmission line in NMR probe design and demonstrate that, for a high quality coil, this approach works best when the coil is roughly tuned and matched by fixed elements to the variable segmented transmission line.

2. Design principle

In general, a segmented transmission line matching network consists of any number N of transmission line segments connecting the load to the probe's input cable as shown in Fig. 1. Each segment T_i consists of a transmission line of length l_i, characteristic impedance $Z_{0,i}$ and complex propagation factor $\gamma_i = \alpha_i + j\beta_i$, where α_i is the attenuation constant and $\beta_i = 2\pi/\lambda_i$ is the phase constant with λ_i as the wavelength. Segment T_1 is connected to a load of impedance Z_1, which consists of the RF sample coil or resonator. According to the well-known formula for impedance transformation along transmission lines [16], the impedance Z_2 looking toward the load into segment T_1 is

$$Z_2 = Z_{0,1}\frac{Z_1 + Z_{0,1}\tanh\gamma_1 l_1}{Z_{0,1} + Z_1\tanh\gamma_1 l_1} \tag{1}$$

And in general, the impedance Z_{i+1} is related to Z_i by the formula

$$Z_{i+1} = Z_{0,i}\frac{Z_i + Z_{0,i}\tanh\gamma_i l_i}{Z_{0,i} + Z_i\tanh\gamma_i l_i} \tag{2}$$

Once N is chosen, we can use this chain relation for impedance to calculate a set of transmission line parameters $Z_{0,i}$, l_i and γ_i for $i = 1, \ldots, N$ so that $Z_{N+1} = Z_0$, the characteristic impedance of the input cable. Rather than proceed in this way, for reasons that will become clear later, we prefer to work with reflection coefficients ρ_i looking into the ith segment towards the load:

$$\rho_i = \frac{Z_i - Z_0}{Z_i + Z_0} \tag{3}$$

Note that these are not the actual reflection coefficients between the transmission line segments, but rather the reflection coefficients that would be obtained if each segment were connected to directly to the input cable. Combining Eqs. (2) and (3) gives a chain relation linking the reflection coefficients at ith and the $i+1$th node:

$$\rho_{i+1} = -\frac{(Z_0^2(1+\rho_i) - Z_{0,i}^2(1-\rho_i))\tanh(\gamma_i l_i) - 2\rho_i Z_{0,i} Z_0}{(Z_0^2(1+\rho_i) + Z_{0,i}^2(1-\rho_i))\tanh(\gamma_i l_i) + 2Z_{0,i} Z_0} \tag{4}$$

Solutions to the equation $\rho_{N+1} = 0$, expanded using (4), describe segmented transmission lines that tune and match the RF sample coil to the input cable.

Our design is shown in Fig. 2a and consists of a coaxial tube into which two dielectric slugs of dielectric constant ε_r have been inserted. The empty coaxial tube has a characteristic impedance of Z_0, equal to the impedance of the input cable, so that there are four electrically different segments T_1 through T_4. Segments T_1 and T_3 have the same characteristic impedance Z_0 as the input cable. Assuming that the same dielectric material is used in segments T_2 and T_4, their characteristic impedance will be reduced from that of the empty tubes by a factor of $\sqrt{\varepsilon_r}$ as given by the standard formula for characteristic impedance in ohms of coaxial transmission lines [16]:

$$Z_{0,2} = Z_{0,4} = \frac{59.95}{\sqrt{\varepsilon_r}}\ln\frac{d_{out}}{d_{in}} \tag{5}$$

where d_{out} and d_{in} are the shield and inner conductor diameter, respectively. We can see from Eq. (5) that $Z_{0,2} = Z_{0,4} = Z_0/\sqrt{\varepsilon_r}$.

The problem of impedance matching is equivalent to obtaining a zero reflection coefficient ρ_5 between segment T_4 and the input cable. We solve this by using the chain relation Eq. (4) to express the relationships between the reflection coefficients. We begin by generating from Eq. (4) the transformations produced by T_1 and T_3:

$$\rho_2 = \rho_1 e^{-2j\beta l_1} \tag{6}$$

$$\rho_4 = \rho_3 e^{-2j\beta l_3} \tag{7}$$

where $\beta = 2\pi/\lambda_{air}$ is the propagation constant of electromagnetic wave in the air, and we neglect transmission line loss so that $\gamma_1 = \gamma_3 \approx j\beta$. Note that these lengths l_1 and l_3 of T_1 and T_3 are adjustable. The second and the fourth transmission line segments are quarter wave dielectric slugs ($\gamma_2 l_2 \approx j\pi/2$ and $\gamma_4 l_4 \approx j\pi/2$) with characteristic impedance $Z_{0,2} = Z_{0,4} = Z_0/\sqrt{\varepsilon_r}$, so Eq. (4) yields:

$$\rho_3 = -\frac{(\rho_2+1) + (\rho_2-1)/\varepsilon_r}{(\rho_2+1) - (\rho_2-1)/\varepsilon_r} \tag{8}$$

$$\rho_5 = -\frac{(\rho_4+1) + (\rho_4-1)/\varepsilon_r}{(\rho_4+1) - (\rho_4-1)/\varepsilon_r} \tag{9}$$

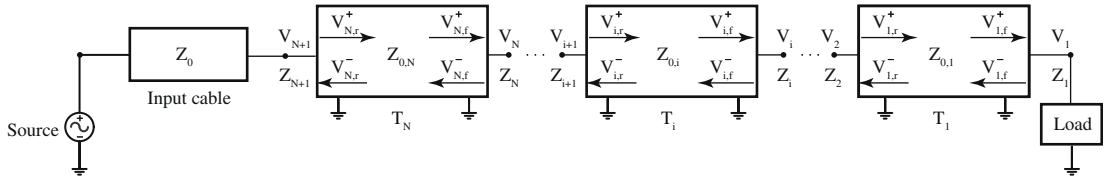

Fig. 1. Block diagram of a generalized segmented transmission line. The power is transmitted to the system via a cable with characteristic impedance Z_0 and further transmitted to the load via N transmission line segments $T_1 \ldots T_N$. The ith segment T_i has a length of li and a characteristic impedance of $Z_{0,i}$. At the front of the ith segment (the end closer to the load), the forward voltage is $V_{i,f}^+$ and the backward voltage is $V_{i,f}^-$. At the rear of the ith segment (the end closer to the input), the forward voltage is $V_{i,r}^+$ and the backward voltage is $V_{i,r}^-$. The total voltage at the ith node is V_i and the transformed impedance at this point is Z_i.

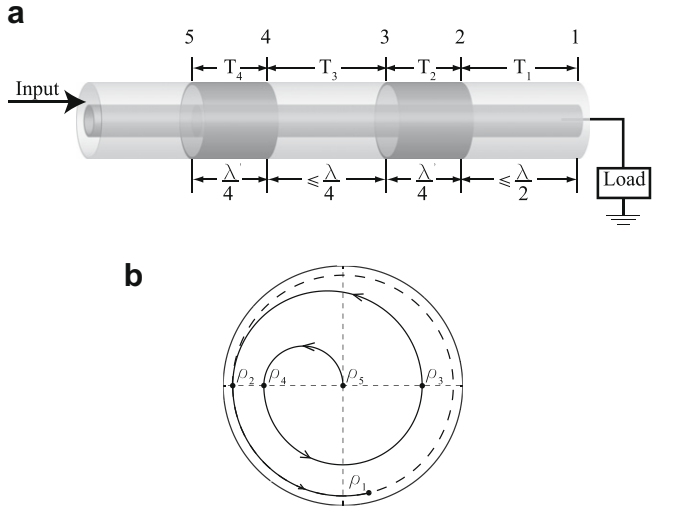

Fig. 2. (a) Schematic view of the four-segment transmission line. The coaxial line has two quarter wave dielectric slugs inside which can freely slide. Segments T_2 and T_4 contain the quarter wave dielectrics slugs, while T_1 and T_3 are adjustable in lengths. As long as the load reflection coefficient satisfies certain requirements, a broad range of impedance can be matched by the proper choice of T_1 and T_3 lengths. (b) The graphical representation of impedance transformation on a polar plot of the reflection coefficient, neglecting transmission line loss. We start from the matched node 5 and deduce the required impedance at the preceding nodes along the forward wave direction (the direction along the arrow). This corresponds to a counter clockwise rotation along the transformation trajectory that starts from the center of polar plot. By going through the low-impedance quarter wave segment T_4, the impedance is transformed to node 4 where the magnitude of the reflection coefficient is increased. This magnitude will remain constant along the circle from 4 to 3, and increase again from 3 to 2. Subsequent transformation from 2 to 1 requires that the load impedance Z_1 lies on the same dashed circle as Z_2. This circle defines the boundary of load impedance that is accessible by four-segment transmission line.

Eqs. (6)–(9) form a complete description of our segmented transmission line matching network, and we can combine them to obtain the analytical solution for l_1 and l_3. Setting $\rho_5 = 0$ in Eq. (9) we derive for ρ_4:

$$\rho_4 = \frac{1-\varepsilon_r}{1+\varepsilon_r} \tag{10}$$

Combining Eq. (10) with Eq. (7) we obtain for ρ_3:

$$\rho_3 = \left(\frac{1-\varepsilon_r}{1+\varepsilon_r}\right) e^{2j\beta l_3} \tag{11}$$

Combining Eq. (11) with Eq. (8) we obtain for ρ_2:

$$\rho_2 = -\frac{(\varepsilon_r^2-1)(e^{j2l_3\beta}-1)}{-(\varepsilon_r+1)^2+(\varepsilon_r-1)^2 e^{j2l_3\beta}} \tag{12}$$

By inspection of Eq. (6), we can see that ρ_1 and ρ_2 will differ by a phase angle but will always have the same magnitude. Rather than substituting (12) into (6) to determine l_3 and l_1 simultaneously, we can simply require that ρ_1 and ρ_2 have the same magnitude. Substituting (12) into $\rho_2\rho_2^* = |\rho_1|^2$ results in the following equation for l_3:

$$\sin(l_3\beta) = \pm\frac{2|\rho_1|\varepsilon_r}{(\varepsilon_r^2-1)\sqrt{1-|\rho_1|^2}} \tag{13}$$

We can see that values of l_3 that will match the probe exist only if the right hand side of Eq. (13) is between -1 and 1, as discussed further below. If there are solutions for $l_3\beta$, we can see that the smallest will lie between 0 and $\pi/2$. Combining Eqs. (6), (12), and (13), and expanding the load reflection coefficient ρ_1 into $|\rho_1|e^{j\theta}$, we find that l_1 can be obtained from:

$$\cos(\theta - 2l_1\beta) = -\frac{(\varepsilon_r^2+1)|\rho_1|}{\varepsilon_r^2-1} \tag{14}$$

As for Eq. (13), a solution exists for Eq. (14) only if the absolute value of right hand side is no larger than unity. It is also clear from inspection that the smallest solution for $\theta - 2l_1\beta$ will be between $\pi/2$ and π.

In the above analysis, we have derived equations for the lengths l_1 and l_3 of our four element segmented transmission line in terms of the load reflection coefficient and the relative dielectric constant of the slugs. We can draw two additional conclusions from Eqs. (13) and (14). First, the requirement that the right hand sides are less than unity means that the four element segmented transmission line is only capable of matching loads for which

$$|\rho_1| \leqslant \frac{\varepsilon_r^2-1}{\varepsilon_r^2+1}. \tag{15}$$

Slugs with larger dielectric constants will be able to match a wider range of loads. Highly reflective loads will need to have $|\rho_1|$ initially reduced by fixed capacitors or inductors, but a segmented transmission line can be used effectively as the adjustable component. Second, we can determine the length L in free-space wavelengths λ_{free} of an adjustable transmission line of the type in Fig. 2a that can match all loads within the limit given by Eq. (15). We have seen that l_1 is never more than $\lambda_{free}/2$, and l_3 is never more than $\lambda_{free}/4$. The two dielectric slugs each have a length of $\lambda_{free}/4\sqrt{\varepsilon_r}$. So the total length of the adjustable line is

$$L = \lambda_{free}\left(\frac{3}{4} + \frac{1}{2\sqrt{\varepsilon_r}}\right). \tag{16}$$

Adjustable slugs with a larger dielectric constant will lead to a shorter adjustable line, but never less than $3\lambda_{free}/4$. For NMR probes, it is clear that the adjustable transmission line will be most useful when L is less than the overall length of the RF probe, so that the adjustable line fits completely into the probe.

It may be instructive to consider the impedance matching process of the segmented transmission line from the familiar perspective of the reflection coefficient. For purposes of this discussion, we will start from the matched impedance at the input port ($\rho_5 = 0$), and move along the segmented transmission line toward the load, ending up at ρ_1. This corresponds to a counter clockwise rotation along the transformation trajectory that starts at the center of Fig. 2b. We assume that ρ_1, the reflection coefficient of the NMR resonator, lies on the edge of the disk defined by Eq. (15). The goal is to move from the origin all the way out to ρ_1 at the limit of the matching range of the four-segment transmission line. The first step is the low-impedance quarter wave segment T_4, which increases the magnitude of the reflection coefficient to a negative real value ρ_4. The next segment, T_3, has the same characteristic impedance as the input cable, so it transforms only the phase of the reflection coefficient to a positive real value ρ_3. In this case, the length of T_3 is one quarter wave, which, as indicated by Eq. (13), is required to match the largest values of $|\rho_1|$. The low-impedance quarter wave segment T_2 again increases the magnitude of the reflection coefficient to ρ_2. Subsequent transformation along the dashed circle to ρ_1 is carried out by segment T_1. The radius of the dashed circle, indicating the largest value of $|\rho_1|$ that can be matched by the four-segment transmission line, is given by Eq. (15).

As seen above, a segmented transmission line matching network uses a series of mismatched transmission lines to transform the impedance of an NMR resonator to the characteristic impedance of the spectrometer. These local mismatches lead to standing waves on the transmission line segments that contribute additional loss to the probe. While a full consideration of loss in segmented transmission line networks is beyond the scope of this

paper, we did carry out a numerical evaluation to estimate the loss from standing waves in our prototype network. Here, we briefly illustrate how to set up the problem. For the loss calculation, it is more convenient to define the reflection coefficient with respect to $Z_{0,i}$, the complex characteristic impedance of the ith transmission line, than to the characteristic impedance of the input cable as in Eq. (3). To emphasize the difference, we designate this reflection coefficient ρ'_i.

$$\rho'_i = \frac{Z_i - Z_{0,i}}{Z_i + Z_{0,i}} \tag{17}$$

For correct evaluation of the loss, it important not to neglect the imaginary part of the characteristic impedance [17], and so we use the use the complex form:

$$Z_{0,i} = \sqrt{\frac{j\omega L_i + R_i}{j\omega C_i + G_i}} \tag{18}$$

where L_i, C_i, R_i, and G_i are the distributed inductance, shunt capacitance, resistance and shunt conductance of the ith transmission line segment. We will also need to use the complex form of the phase constant, $\gamma_i = \alpha_i + j\beta_i$ where attenuation α_i is no longer zero.

Referring to Fig. 1, the total voltage at the $(i+1)$th node V_{i+1} can be related to the incident voltage at the ith node V_i^+ by the following relation:

$$\begin{aligned} V_{i+1} &\equiv V_{i,r}^+ + V_{i,r}^- \\ &= V_{i,f}^+ \exp(\gamma_i l_i) + V_{i,f}^- \exp(-\gamma_i l_i) \\ &= V_{i,f}^+ \exp(\gamma_i l_i) + \rho'_i V_{i,f}^+ \exp(-\gamma_i l_i) \end{aligned} \tag{19}$$

And the total voltage at the $(i+1)$th node V_{i+1} can also be expressed as:

$$\begin{aligned} V_{i+1} &\equiv V_{i+1,f}^+ + V_{i+1,f}^- \\ &= V_{i+1,f}^+ + \rho'_{i+1} V_{i+1,f}^+ \end{aligned} \tag{20}$$

V_1 the voltage across the load, can be obtained in terms of the known incident voltage V_5^+ by repetitive use of the chain relation from Eqs. (19) and (20). The power efficiency (PE) of the segmented transmission line is just the ratio of the power dissipated in the load versus the incident power from the input cable:

$$PE = \frac{Re\left(\frac{|V_1|^2}{Z_1^*}\right)}{Re\left(\frac{|V_5^+|^2}{Z_0^*}\right)} \tag{21}$$

Numerical evaluation of the power efficiency for a given load impedance using Eq. (21) is straightforward as long as the propagation constants of the transmission line segments are known.

3. Experiments

To demonstrate the design principle proposed in this paper, we incorporated the segmented transmission line into the VAS probe that was designed and built in the lab of R.W. Martin for a 500 MHz wide bore magnet [15]. This probe employs a double frequency resonator that is capacitively coupled to the main circuit by four coaxial capacitors. The coaxial capacitors are utilized to achieve contactless power transfer between the stationary tuning circuit and mobile sample coil so that a robust electric junction can be achieved for variable angle spinning and switched angle spinning experiments. Originally, both ^{1}H and ^{13}C channels were impedance matched by an L-network consisting of a transmission line with a single movable dielectric slug and a shunt variable capacitor as shown in Fig. 3a. This L-network, based on a tuning structure found in a Bruker Biospin probe, can be analyzed following a similar approach to that outlined in the "Design Principle" section. The L-network for the ^{1}H channel was later replaced with an adjustable segmented transmission line using dual quarter-wave slugs as shown in Fig. 3b. The impedance of the probe was measured for a set of four frequencies both with and without a sample, and Eqs. (13) and (14) were used to predict the positions of the slugs required to match this impedance to 50 Ω.

The four-segment transmission line was constructed by inserting two dielectric cylinders into a rigid coaxial line. Both the inner and outer tubes of the coaxial line were made of OFHC copper tubing. The outer tube has an OD of 0.625 inch and an ID of 0.571 inch, while the inner rod has an OD of 0.25 inch. These particular dimensions were chosen so that the empty coaxial line would have a characteristic impedance of approximately 50 Ω, equal to the system impedance of the spectrometer. The two dielectric slugs were fabricated from Macor (Corning, Inc.), a ceramic material chosen for its machinability. The slugs were fabricated with an OD of 0.564 in. and an ID of 0.254 in., which gave them enough clearance within the copper tubes to move freely up and down. To allow quantitative comparison with Eqs. (13) and (14), the slugs should be exactly one quarter wave length at the operating frequency of 500 MHz. For Macor, the relative dielectric constant $\varepsilon_r \approx 5.7$ [18]. However, the gaps that allow free motion of the slugs reduce the effective dielectric constant of the relevant segments. We can take into account the effect of the two gaps on the capacitance per unit length of the cable by treating the gaps and the dielectric cylinder as three coaxial capacitors in series. Using the standard expression for the capacitance of the coaxial cylinders [19], the resulting effective dielectric constant ε_{eff} can be defined using the expression:

$$\ln\frac{R_a}{R_{in}} + \frac{1}{\varepsilon_r}\ln\frac{R_b}{R_a} + \ln\frac{R_{out}}{R_b} = \frac{1}{\varepsilon_{eff}}\ln\frac{R_{out}}{R_{in}} \tag{22}$$

where R_{out} is the radius of the shield, R_{in} the radius of the inner tube, R_b and R_a are the outer and inner radii of the dielectric slug, respectively. For the dimensions above, $\varepsilon_{eff} = 4.9$. The length of the quarter wave slug must then be 6.8 cm, about 8% longer than would have been obtained without the gaps. The slugs were cut to this length and inserted into the copper tubes. As shown in Fig. 3c, the position of each dielectric slug is adjusted independently by a brass 6–32 threaded rod placed parallel to the line (Fig. 3c). The threaded rod drives a position controlling unit made of G-10 fiberglass laminate which is connected to the dielectric slug. The entire coaxial tube is 0.6 m in length. Because the dielectric slug is much larger than the G-10 screw, and because the electromagnetic field inside the coaxial line is only minimally affected by the 1/8"' slots on its outer cylinder, the mechanical system is expected to have negligible influence on the impedance properties of transmission line.

To verify its operation, and to test the validity of Eqs. (13) and (14), the adjustable segmented transmission line was used to tune and match the probe at a set of four frequencies both with and without a sample. The sample used for these tests was a 4 mm zirconia rotor filled with 20 μL of 2% H_2O/D_2O. To accurately obtain the load impedance needed to calculate the required slug positions, the two dielectric slugs were removed from the coaxial line and a vector network analyzer was used to directly read out the unmatched impedance at the probe's input. The load impedance was calculated based on the known transmission line length using Eq. (1). Next, the dielectric slugs were inserted and their positions empirically adjusted to minimize the voltage reflection at the probe's input. Table 1 gives the measured lengths of transmission line segments required to match the probe under the above conditions and the predictions based on Eqs. (13) and (14), as well as the load measurements expressed both as impedance and reflection coefficient. Good agreement was found, tending to confirm the validity of our theoretical model. We should also note that the segmented transmission line was able to match the probe both with and without the aqueous sample.

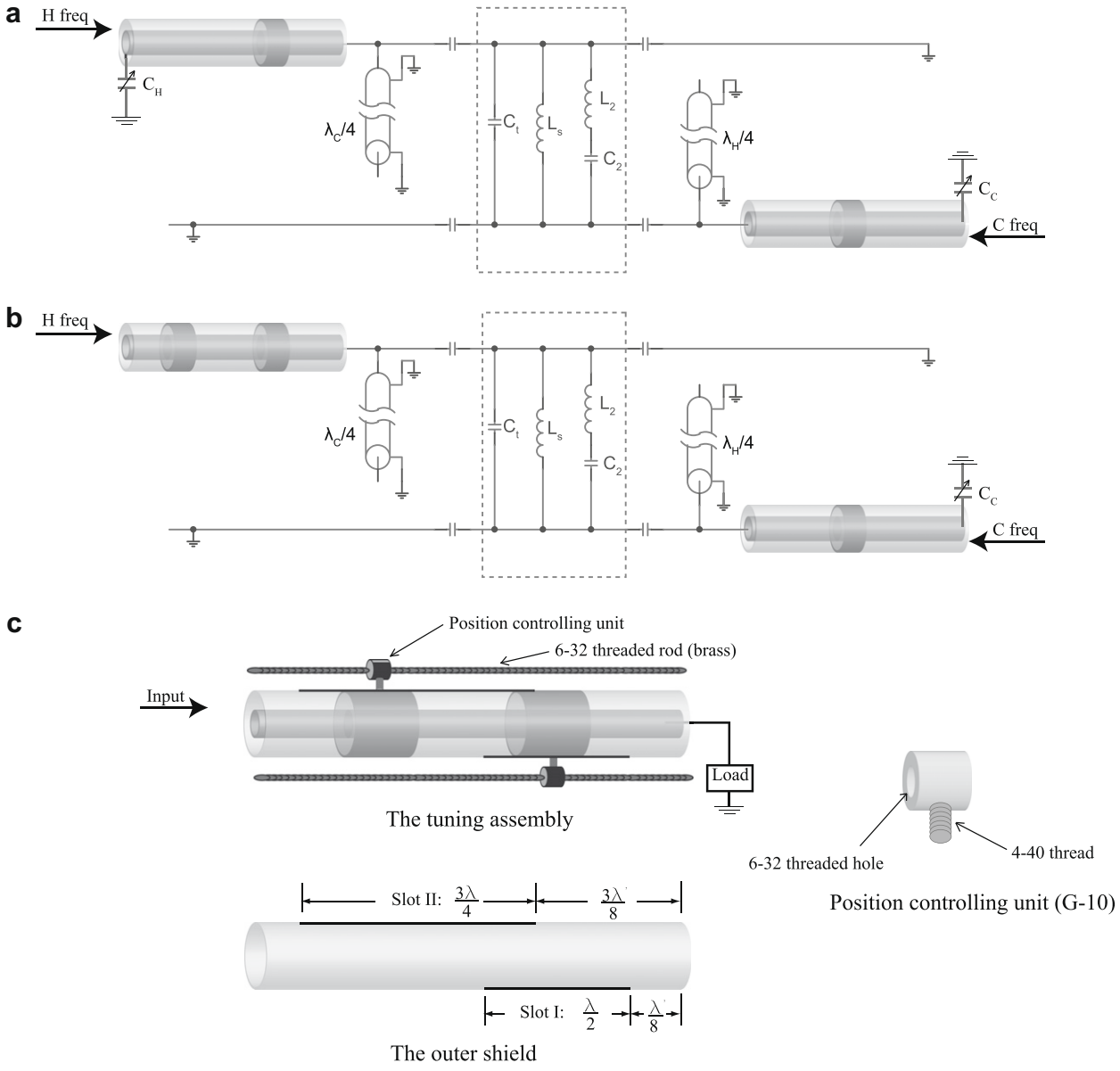

Fig. 3. (a) The circuit diagram of the matching network that was originally used in our Variable Angle Spinning probe. The portion enclosed in the dashed box represents the double frequency resonator that is capacitively coupled to the main circuit. In this original matching network, the proton channel utilizes a single dielectric slug and a shunt capacitor. But in (b), the proton channel is matched by a two-slug segmented transmission line. A pair of dielectric slugs are inserted into a single uniform coaxial line and no parallel capacitor is required. (c) The schematic representation of the mechanical system used for position adjustment. Each dielectric slug is connected to a position controlling unit in the center. Each position controlling unit consists of a 6–32 threaded collar into which a short 4–40 threaded rod is mounted. This threaded rod connects to the dielectric slug through a 1/8" wide slot on the outer cylinder of the coaxial transmission line. The bottom figure shows the slot positions. It is important to leave enough intact surface at both ends of the outer tube to preserve the mechanical integrity.

Table 1
The predicted and measured lengths of transmission line segments T_1 and T_3 to match the load impedance. T_2 and T_4 are both quarter wave dielectric slugs (67.8 mm each). The load is a capacitively coupled LC resonator.

	Freq	Load	Reflection	T_1 (mm)		T_3 (mm)	
	MHz	Impedance (Ω)	Coefficient	Predict	Actual	Predict	Actual
With sample	499	94.8 + 100.8i	0.535 + 0.324j	214.7	216	33.6	33
	500	184.4 + 14.2i	0.575 + 0.026j	195.1	195	29.4	29
	501	102.9 − 79.8i	0.486 − 0.268j	170.3	170	27.7	27
	502	44.5 − 66.2i	0.290 − 0.498j	142.7	143	29.1	29
Without sample	499	31.1 + 78.4i	0.362 + 0.616j	231.5	232	43.4	43
	500	69.4 + 100.2i	0.509 + 0.413j	219.2	220	36.4	36
	501	163.7 + 72.3i	0.580 + 0.142j	202.6	202	31.1	31
	502	144.3 − 67.4i	0.541 − 0.159j	180.2	180	28.3	28

We found that moving the two dielectric slugs together is similar to adjusting the tuning capacitor in a conventional network, and moving the bottom slug (T_4) with the top one fixed is similar to adjusting the matching capacitor. As is the case in a conventional network, the "tuning" and "matching" are not completely independent, and several iterations are required to minimize the reflected voltage.

We also compared the power efficiency of the two different matching circuits. The probe's input power was determined from the peak-to-peak voltage (V_{p_p}) displayed on a 1 GHz digital phosphor oscilloscope that was connected to the input cable via a 50 dB directional coupler. The power value was then calculated from the following equation:

$$\text{Power} = \frac{10^5 V_{p-p}^2}{400} \tag{23}$$

where "V_{p_p}" is in units of volts and "Power" is in units of watts. When the proton channel was matched by the L-network shown in Fig. 3a, the 90° time was measured to be 4.65 μs with 22.9 watts of input power. In comparison, when the proton channel was matched by the segmented transmission line shown in Fig. 3b, the 90° time was 4.3 μs with the same input power level. This corresponds to a 8% increase of B_1 field or a 17% increase of power efficiency. We believe the improved efficiency comes from the fact that the four-segment transmission line does not have loss from the branching capacitor or soldering junction present in the L-network.

To further explore the question of power efficiency, we performed a numerical simulation for the 500 MHz prototype segmented transmission line using the method proposed in the "Design Principle" section. A conductivity of 5.998×10^7 S/m was assumed for the inner and outer copper tubes, and a value of 4.7×10^{-3} for the loss tangent of the Macor dielectric slugs [14]. For each possible load reflection coefficient, the lengths of T_1 and T_3 were numerically optimized to minimize the reflected power at the input port. The results are shown in Fig. 4a and b. For reflection coefficients within the circle defined by Eq. (15), where a perfect match is possible, the lengths of T_1 and T_3 calculated from the analytical solutions Eqs. (14) and (13) exactly matched the numerical simulation. As predicted from the analytical derivation, Fig. 4a indicates that T_1 is always shorter than half a wavelength. And it is interesting to notice that T_1 strongly depends on the phase of the reflection coefficient. On the other hand, Fig. 4b shows the optimal value of T_3 to be smaller than quarter a wavelength and independent of the phase of the load reflection coefficient. The different roles of T_1 and T_3 can be understood from the graphic representation of impedance transformation of Fig. 2b. The predicted power efficiency at 500 MHz is shown in Fig. 4c. Better than 80% power

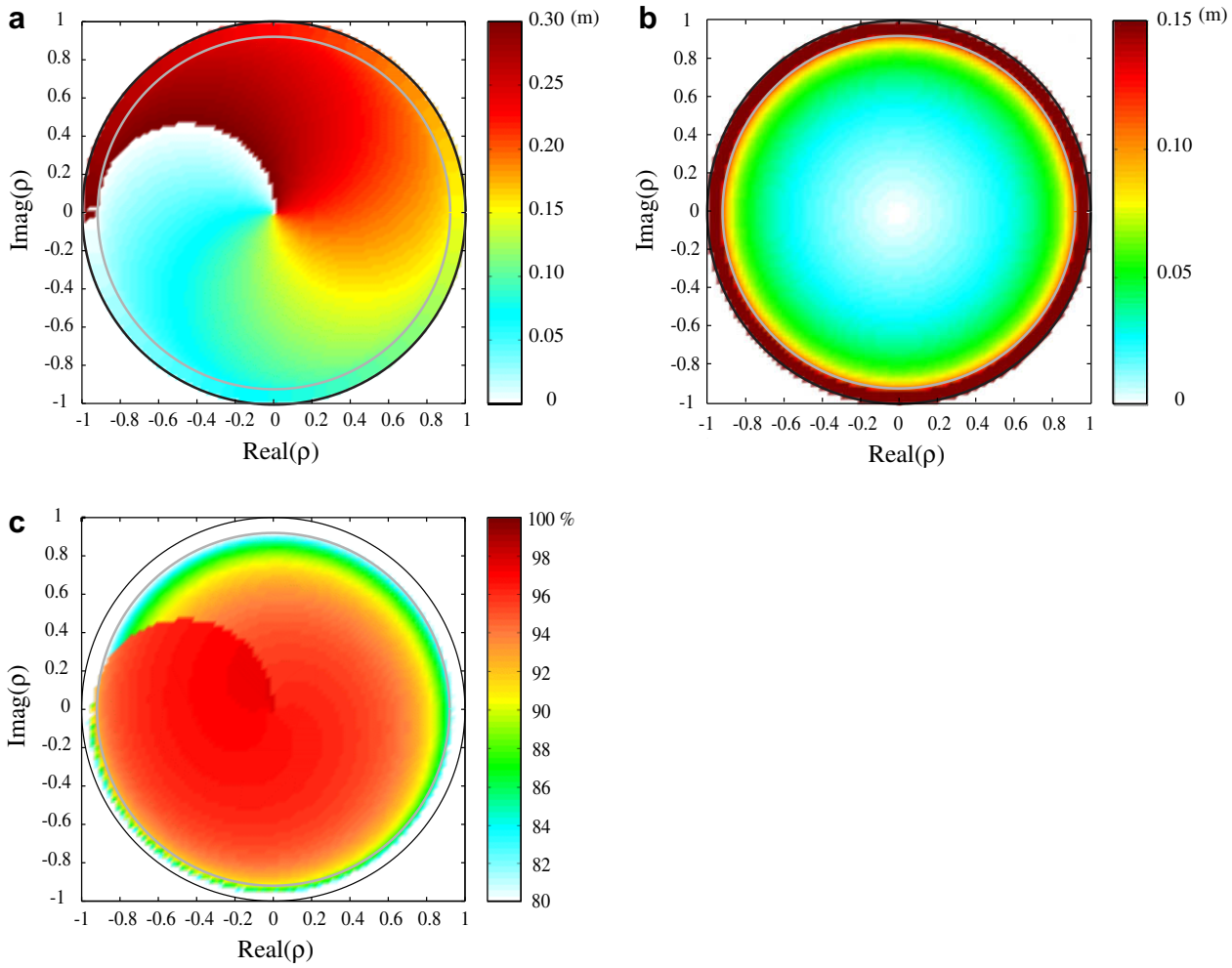

Fig. 4. Polar plots of the required lengths and efficiency of the segmented transmission line matching network as a function of load reflection coefficient *r*. Values were calculated by numerical simulation for the known parameters of the segmented transmission line built for the 500 MHz prototype probe. (a) T1 length and (b) T3 length in meters required to minimize the probe's overall reflection coefficient. (c) The efficiency for the optimal length configuration. This figure only shows the contour level higher than 80%. In all figures, the grey circle is the maximum reflection circle defined by Eq. (15).

efficiency was predicted for the entire range within the maximum reflection circle. All of the measured values of reflection coefficient from Table 1 fall well within the maximum reflection circle, and so they can all be expected to have good power efficiency.

While Macor was chosen for the prototype because it is easily machinable using standard tools, it does have a loss tangent (4×10^{-3}) that is significantly greater than other ceramics that might be used for slugs. The loss calculation was repeated for slugs having the dielectric constant of Macor but a loss tangent of 2×10^{-4}, comparable to that of alumina. The calculated efficiency of the segmented transmission line improved from 80% to 97%, indicating that most of the loss in the line comes from the dielectric and not the resistivity of the copper conductors.

4. Conclusion and discussion

The adjustable segmented transmission line utilizes the multiple reflections between each segment to achieve overall impedance matching at the input port. Because there are no sliding contacts on the transmission line, this kind of tuning network should have excellent durability. By empirically adjusting the position of its two quarter wave slugs both inductive and capacitive loads can be matched. Because highly reflective loads such as copper solenoids cannot be completely matched with the network, it works best when employed along with a network of fixed series and parallel capacitors to reduce the reflection coefficient. Such a configuration is embodied in a prototype 500 MHz VAS probe for which the adjustable transmission line is used to tune and match the ^{1}H channel. This probe has been used for the past 2 years in Dr. R.W. Martin's lab in UC-Irvine for variable angle spinning experiments on liquid crystals.

In this paper, we mainly dealt with the issue of the accessible range of load impedance. In practice, a spectroscopist is typically more concerned with the frequency range over which a particular probe can be tuned. The range depends both on the dielectric constant of the tuning slugs through Eq. (15) and on the frequency dependence of the load impedance. For the case of the 500 MHz VAS probe, the segmented transmission line can match all loads with reflection coefficients $|\rho_1| < 0.92$. The capacitively coupled resonator was measured to have a reflection coefficient less than 0.9 within the range 490–510 MHz with and 492–512 MHz without the sample. The observed tuning range was in good agreement. Although the dielectric slugs are designed to match the greatest range of load impedance at a particular frequency, the adjustable line can actually be used over a reasonable frequency range. A graphical analysis based on Fig. 2 indicates that slugs either shorter or longer than a quarter wave will result in a maximum reflection circle of smaller radius. For example, for 470 MHz (the ^{19}F frequency), the radius is reduced from 0.920 to 0.919. This result indicates that the segmented transmission line has a broad frequency range, as long as the load impedance falls within the maximum reflection circle of the matching network. To match a load with a reflection coefficient of arbitrary phase, the lengths of the gaps T_1 and T_3 should be adjustable up to a half and a quarter wavelength, respectively. In order to ensure that the loads of any phase can be matched over the probe's complete frequency range, the segment length required should be derived from the lowest frequency at which the probe will be used.

Although the present paper describes an application of the adjustable segmented transmission line for solid state NMR, it may have utility in other areas of magnetic resonance, particularly where a single tuning network is needed that can accommodate a great range of load impedance. An example of such an application may be probes for magnetic resonance imaging that are highly loaded, and so are subject to large shifts in load impedance by the range of possible samples or patients.

Acknowledgments

This work has been supported by the National High Magnetic Field Laboratory through Cooperative Agreement (DMR-0084173) with the National Science Foundation and the State of Florida. The authors thank Prof. Rachel W. Martin for granting us access to her 500 MHz spectrometer in the chemistry department of UC-Irvine. Special thanks to Dr. Samuel Grant, Dr. Xiaozhong Zhang, Dr. Wurong Zhang, and Mr. Peter Gor'kov for their helpful comments and suggestions. C.Q. is grateful for financial support from Bruker Biospin Inc.

References

[1] D.D. Traficante, Maximum power transfer and percent efficiency: which is more important, Concept. Magn. Reson. 9 (1997) 13–16.
[2] I. Viohl, G.T. Gullberg, Tuning and matching networks for MR-imaging and spectroscopy, J. Magn. Reson. Imag. 4 (1994) 627–630.
[3] Q.W. Zhang, H.M. Zhang, K.V. Lakshmi, D.K. Lee, C.H. Bradley, R.J. Wittebort, Double and triple resonance circuits for high-frequency probes, J. Magn. Reson. 132 (1998) 167–171.
[4] Y. Li, T.M. Logan, A.S. Edison, A. Webb, Design of small volume HX and triple-resonance probes for improved limits of detection in protein NMR experiments, J. Magn. Reson. 164 (2003) 128–135.
[5] S.P. Graether, J.S. DeVries, R. McDonald, M.L. Rakovszky, B.D. Sykes, A H-1/F-19 minicoil NMR probe for solid-state NMR: application to 5-fluoroindoles, J. Magn. Reson. 178 (2006) 65–71.
[6] S.M. Holl, R.A. Mckay, T. Gullion, J. Schaefer, Rotational-echo triple-resonance NMR, J. Magn. Reson. 89 (1990) 620–626.
[7] V.R. Cross, R.K. Hester, J.S. Waugh, Single coil probe with transmission-line tuning for nuclear magnetic double-resonance, Rev. Sci. Instrum. 47 (1976) 1486–1488.
[8] J.A. Stringer, G.P. Drobny, Methods for the analysis and design of a solid state nuclear magnetic resonance probe, Rev. Sci. Instrum. 69 (1998) 3384–3391.
[9] V.D. Kodibagkar, M.S. Conradi, Remote tuning of NMR probe circuits, J. Magn. Reson. 144 (2000) 53–57.
[10] Y.W. Kim, W.L. Earl, R.E. Norberg, Cryogenic probe with low-loss transmission line for nuclear magnetic resonance, J. Magn. Reson. Ser. A 116 (1995) 139–144.
[11] H.J. Jakobsen, P. Daugaard, E. Hald, D. Rice, E. Kupce, P.D. Ellis, A 4-mm probe for C-13 CP/MAS NMR of solids at 21.15 T, J. Magn. Reson. 156 (2002) 152–154.
[12] R.W. Martin, E.K. Paulson, K.W. Zilm, Design of a triple resonance magic angle sample spinning probe for high field solid state nuclear magnetic resonance, Rev. Sci. Instrum. 74 (2003) 3045–3061.
[13] J.M. Cusack, S.M. Perlow, B.S. Perlman, Automatic load contour mapping for microwave-power transistors, IEEE T. Microw. Theory Tech. MTT-22 (1974) 1146–1152.
[14] M.A. Hamid, M.M. Yunik, On design of stepped transmission-line transformers, IEEE T. Microw. Theory Tech. MTT-15 (1967) 528.
[15] C.Q. Qian, A. Pines, R.W. Martin, Design and construction of a contactless mobile RF coil for double resonance variable angle spinning NMR, J. Magn. Reson. 188 (2007) 183–189.
[16] R. Bansal, Fundamentals of engineering electromagnetics, Third ed., CRC Press Taylor & Francis, Boca Raton, 2003.
[17] L.S. Nergaard, B. Salzberg, Resonant impedance of transmission lines, Proc. Inst Radio Eng. 27 (1939) 579–584.
[18] G.P. Pells, R. Heidinger, A. Ibarrasanchez, H. Ohno, R.H. Goulding, An intercomparison of techniques for measuring dielectric permittivity and loss over a wide frequency-range, J. Nucl. Mater. 191 (1992) 535–538.
[19] S. Ramo, J.R. Whinnery, T. Van Duzer, Fields and waves in communication electronics, third ed., John Wiley and Sons, New York, 1994.